Altered linkage pattern of N-glycan sialic acids in pseudomyxoma peritonei

Pirjo Nummela[1], Annamari Heiskanen[2], Soili Kytölä[3], Caj Haglund[4,5], Anna Lepistö[4], Tero Satomaa[2], and Ari Ristimäki[1,6]*

[1]Applied Tumor Genomics Research Program, Research Programs Unit, University of Helsinki, P.O. Box 63, FI-00014 University of Helsinki, Finland

[2]Glykos Finland Ltd, Viikinkaari 6, FI-00790 Helsinki, Finland

[3]Department of Genetics, HUSLAB, HUS Diagnostic Center, Helsinki University Hospital, P.O. Box 720, FI-00029 HUS, Finland

[4]Department of Surgery, University of Helsinki and Helsinki University Hospital, P.O. Box 440, FI-00029 HUS, Finland

[5]Translational Cancer Medicine Research Program, Research Programs Unit, University of Helsinki, P.O. Box 63, FI-00014 University of Helsinki, Finland

[6]Department of Pathology, HUSLAB, HUS Diagnostic Center, University of Helsinki and Helsinki University Hospital, P.O. Box 400, FI-00029 HUS, Finland

*To whom correspondence should be addressed: Ari Ristimäki, Pathology, HUSLAB, P.O. Box 400, FI-00029 HUS, Finland. Phone: 358-0-4711; Fax: 358-2941-26700; E-mail: ari.ristimaki@helsinki.fi

Running title: Sialic acid linkage pattern in pseudomyxoma peritonei

Supplementary data included: Supplementary Tables I-III, Supplementary Figures 1-4

Abstract

Pseudomyxoma peritonei (PMP) is a highly mucinous adenocarcinoma growing in the peritoneal cavity and most commonly originating from the appendix. Glycans play an important role in carcinogenesis and glycosylation is altered in malignant diseases, including PMP. We have previously demonstrated that fucosylation of N-glycans is increased in PMP, but we did not observe modulation of overall sialylation. As sialic acids can be attached to the rest of the glycan via α2,3- or α2,6-linkage, we have now analyzed the linkage patterns of sialic acids in tissue specimens of normal appendices, low-grade appendiceal mucinous neoplasms (LAMN), low-grade (LG) PMP, and high-grade (HG) PMP. For the linkage analysis, the enzymatically released acidic N-glycans were first treated with ethyl esterification or α2,3-sialidase digestion followed by MALDI-TOF mass spectrometry. Significant increase in the relative abundance of α2,6-sialylated and decrease in α2,3-sialylated N-glycans was observed in PMP tumors as compared to the normal appendices ($P < 0.025$). More specifically, increased α2,6-sialylation ($P < 0.05$) and decreased α2,3-sialylation ($P < 0.01$) was detected in afucosylated and monofucosylated N-glycans of PMPs, whereas the less abundant multifucosylated glycans, containing terminal fucose, demonstrated increased α2,3-sialylation ($P < 0.01$). Importantly, the increase in α2,6-sialylation was also detected between PMP and the appendiceal precursor lesion LAMN ($P < 0.01$). The identified glycosylation alterations produce ligands for sialic acid-binding immunoglobulin-like lectins (Siglecs) and sialofucosylated glycans binding selectins, which play a role in the peritoneal dissemination and progression of the disease.

Key words: fucosylation / pseudomyxoma peritonei / sialylation

Words 237

Introduction

Pseudomyxoma peritonei (PMP) is a relatively rare malignancy with an incidence of 3.2 cases per million per year (Patrick-Brown, T D J H et al. 2020). As PMP is a slowly progressing disease, it has been estimated that around 12 000 people lived with PMP in Europe in 2018 (Patrick-Brown, T D J H et al. 2020). PMP appears to be slightly more common in women, even though the probability to find it may just be higher due to symptoms caused by ovarian deposits (Mittal et al. 2017). At early stages, the disease otherwise tends to be asymptomatic. Appendiceal mucinous neoplasms typically appear in the sixth decade of the life, but the age range is quite wide (Misdraji J, Carr NJ, Pai RK 2019). PMP presents as a highly mucinous adenocarcinoma growing in the peritoneal cavity, and it is generally originated from a perforated low-grade appendiceal mucinous neoplasm (LAMN) (Carr et al. 2012). The main characteristic feature of PMP is the abundant secretion of mucinous ascites, which slowly fills the peritoneal cavity and leads to abdominal distension. In the terminal phase of the disease, this causes progressive obstruction of the bowel, finally leading to the death of the patient. The more common low-grade (LG) subtype of PMP mostly spreads on the surfaces of peritoneal cavity, whereas the high-grade (HG) subtype invades surrounding tissues and organs, thereby shortening the survival time when compared to the LG subtype (overall 5-year survival 23% for HG and 63% for LG) (Carr et al. 2012). At present, the optimal treatment of PMP consists of cytoreductive surgery, followed by hyperthermic intraperitoneal chemotherapy (HIPEC) targeting residual tumor cells (Sugarbaker et al. 1987). After this combinatory therapy, the 5-year survival has been reported to be 77% for LG and 53% for HG PMP (Järvinen et al. 2014). Targeted therapies would be desirable to further improve the survival of especially HG tumor bearing patients. Moreover, as PMP patients can live 20 years with the slowly progressing LG tumor, targeted therapies merely reducing the mucus production could improve the patients' quality of life. Molecular studies of this rare but lethal disease are thus essential.

Knowledge of the genomic background of PMP has greatly increased during the last decade. PMP tumors are microsatellite stable (Kabbani et al. 2002; Nummela et al. 2015) and their mutation profile presents two common mutations, *KRAS* and *GNAS*, reported in 58-100% and 40-100% of the cases, respectively (Nummela et al. 2015; Bignell et al. 2016; Saarinen et al. 2017). Shetty et al. have reported prognostic value

for p53 immunohistochemistry in PMP (Shetty et al. 2013), and we have shown aberrant p53 immunostaining to be more frequent in HG than LG PMP (31.3% vs. 7.1%, respectively) and to associate with worse outcome (Nummela et al. 2015).

In addition to cancer-related gene mutations, aberrant glycosylation can serve as a driver of malignant behavior, and glycans play a critical role in several important cancer-related cellular functions, such as cell signaling, adhesion, and invasion (Pinho and Reis 2015; Mereiter et al. 2019). The most common alterations in the N-glycans of gastrointestinal cancers include changes in glycan branching, and increase in fucosylation and sialylation (Mereiter et al. 2016). Along with enabling cancer cells to modulate their behavior, altered glycosylation products are important biomarkers for cancer diagnostics. An excellent example is tumor marker CA19-9 (sialyl-Lewis a), which is a sialylated and fucosylated glycan structure used in the diagnosis and follow-up of pancreatic and gastrointestinal cancer patients, including PMP patients. Further, aberrantly expressed cell-surface glycans can be utilized as targets for glycan-directed antibody-drug conjugates in antitumor therapy (Cox et al. 2019).

Sialic acids, derivatives of neuraminic acid, are widespread acidic modifications of glycans. The most common sialic acid among human glycans is N-acetylneuraminic acid (Neu5Ac), but altogether over 50 natural derivatives of neuraminic acid are known (Li, F. and Ding 2019). Sialic acids typically occur in the terminal position of N- and O-linked glycans and are linked to the rest of the glycan structure via an α2,3- or an α2,6-linkage, depending on the specificity of the sialyltransferase enzyme performing the attachment. At physiological pH, sialic acids are negatively charged and these terminal negative charges of glycans are able to affect many features of the glycoprotein itself, including its conformation, oligomerization, as well as interaction with other proteins (Li, F. and Ding 2019). Further, sialic acids can themselves bind to specific lectins, such as sialic acid-binding immunoglobulin-like lectins (Siglecs) and selectins (binding sialofucosylated glycans) (Bhide and Colley 2017; Mereiter et al. 2019). In contrast to sialic acid, the deoxyhexose sugar L-fucose is a neutral glycan constituent, which may occur either in the terminal portion of N- and O-linked glycans (terminal or complex fucosylation) or in the core structure of N-glycans (core fucosylation) (Schneider et al. 2017; Keeley et al. 2019). The linkage type here may be an α1,6- (core

fucose), α1,2-, α1,3-, or α1,4-linkage (terminal fucoses), depending on the specificity of the responsible fucosyltransferase. Terminal fucosylation combined with sialylation (sialyl-Lewis antigens) is needed for the binding of selectins mentioned above (Bhide and Colley 2017; Mereiter et al. 2019).

In our previous work, we demonstrated highly increased fucosylation of neutral N-glycans in PMP, but were unable to detect modulation of overall sialylation (Saarinen et al. 2018). Here, we analyzed more specifically the linkage pattern of N-glycan sialic acids in normal appendices, low-grade appendiceal mucinous neoplasms (LAMN), LG PMPs, and HG PMPs. Further, we compared the abundancies of α2,3- and α2,6-linked sialic acids in respect of fucosylation. These linkage analyses revealed significant changes in PMP tumors' sialylation, which may be involved in the peritoneal dissemination and tumor progression.

Results

Sialylation in the glycan profiles

Sialic acid can be attached to the rest of the glycan with an α2,3- or an α2,6-linkage. We analyzed sialic acid linkage pattern by pretreating the acidic N-glycans with ethyl esterification preceding MALDI-TOF mass spectrometry. By this method, the acidic N-glycan profile was separated into α2,3- and α2,6-sialylated monosaccharide compositions, yielding 94 acidic compositions (Supplementary Figure 1 and Supplementary Table I). The largest number of sialylated glycans were monosialylated (75/94 structures), and di- and trisialylated structures were less commonly detected (16/94 and 3/94, respectively). When considering the relative abundancies of these structural subtypes, the mean overall abundance value of monosialylated structures varied in the four sample groups (normal appendices, LAMN, LG PMP, and HG PMP) between 72.9 and 82.5%, that of disialylated ones between 17.3 and 26.5%, and the trisialylated structures were ≤ 0.8% (Supplementary Figure 2A). Due to the considerable abundance of disialylated structures, the possible presence of α2,8-linked sialic acids, occurring in poly-sialic acids, was inspected. Their abundance was, however, estimated to be negligible based on mild periodate oxidation analysis, wherein any α2,8-linked sialic acids would have made the C7-C8 and C8-C9 bonds of the inner sialic acid residue specifically resistant to oxidative cleavage (data not shown). Concerning sialic acid linkages, most of the sialylated glycan signals contained only one type of linkage, either α2,3- or α2,6-linkage (54 and 37 glycans, respectively), and only three glycan signals contained both linkage types (overall abundance ≤ 0.8% in all the specimens) (Supplementary Figure 2B and Supplementary Table I). These low abundance glycans were omitted from the subsequent analyses.

Comparison of structures containing α2,3- or α2,6-sialylation

To compare the structural types showing α2,3- or α2,6-sialylation, we fractioned the monosaccharide compositions into three groups: structures with both α2,3- and α2,6-sialylated forms (shared structures), and structures containing only one type of sialic acid linkage, either α2,3- or α2,6-linkage (unique structures). The shared structures consisted of 26 monosaccharide compositions (Figure 1). Of these structures, S1H5N4F1 showed higher tendency for α2,3-sialylation (except in HG tumors), whereas S1H5N4 and

S2H5N4 clearly favored α2,6-linked sialic acid. Of unique structures, 28 compositions contained α2,3-linkage (Figure 2A), whereas only 11 contained α2,6-linkage (Figure 2B). All these unique structures were, however, quite low abundance structures, most often showing relative abundance below 1%. The only exception was composition S1(2.6)H3N6F2, whose mean relative abundance varied between 1.1 and 4.3%. A common theme in unique structures was, however, the predominance of multifucosylated (F > 1) compositions in α2,3-sialylated structures (18/28; Figure 2A). Indeed, both the subgroups of α2,3- and α2,6-sialylated glycans altogether contained 33 afucosylated or monofucosylated structures, whereas the number of different multifucosylated monosaccharide compositions greatly differed between these subgroups, being 21 for α2,3-sialylated and only four for α2,6-sialylated structures (Supplementary Table I). Three multifucosylated structures (S1H4N4F3, S1H5N4F2, and S1H4N5F2), however, demonstrated both linkage types (Figure 1), and one (S1H3N6F2) was found to contain only α2,6-linked sialic acid (Figure 2B). In unique α2,6-sialylated glycans, several multisialylated structures (S > 1) were, in turn, detected (S2H5N2, G1S2H4N4, S2H5N5F1, S2H6N5, and S3H6N5) (Figure 2B). Indeed, when comparing the relative abundancies of all α2,3- and α2,6-sialylated structures in terms of their sialylation level, α2,6-sialylation seemed to predominate in multisialylated structures (Supplementary Figure 2B).

Sialic acid linkage pattern is modulated in PMP

When we compared the sialic acid linkage patterns of all sialylated N-glycans in our sample groups, normal appendices and LAMNs showed nearly equal proportions of the two linkage types, whereas PMP tumors showed significantly increased proportion of α2,6-sialylated and, correspondingly, decreased proportion of α2,3-sialylated glycans as compared to normal appendices (*P*-values 0.020 and 0.022, respectively). This led to significantly decreased α2,3/α2,6 linkage ratio in PMPs when compared to either control appendices ($P = 0.020$) or LAMNs ($P = 0.004$) (Figure 3A). When the α2,3/α2,6 linkage ratios were further compared between the paired LAMN and LG PMP specimens of the same patients, a strong correlation was found ($R^2 = 0.855$) (Figure 3B).

Changes in sialic acid linkage pattern in respect to fucosylation

As increased fucosylation is a frequent glycosylation alteration in cancer as well, also reported in our previous PMP study (Saarinen et al. 2018), we next analyzed in more detail the co-existence of sialylation and fucosylation in the same glycan structures. First, majority of the sialic acids were indeed detected in afucosylated or monofucosylated glycans, α2,3-sialylation being most abundant in monofucosylated (Figure 4A) and α2,6-sialylation in afucosylated structures (Figure 4B). When we then compared how these structural subtypes changed between control appendices and PMPs, we noticed that in afucosylated and monofucosylated structures α2,3-sialylation decreased (*P*-values 0.001 and 0.009, respectively) and α2,6-sialylation increased (*P*-values 0.043 and 0.036, respectively), whereas in multifucosylated structures α2,3-sialylation increased ($P = 0.006$) (Figure 4). Of note here is that major part of the multifucosylated and α2,6-sialylated subtype was composed of the monosaccharide composition S1(2.6)H3N6F2 (Figure 2B), which is proposed to contain two LacdiNAc (GalNAcβ1,4GlcNAc) glycan units instead of the more common LacNAc (Galβ1,4GlcNAc) unit (see the representative structures depicted in Figure 4). This composition was significantly decreased in PMPs as compared to control appendices (fold change 0.54; $P = 0.044$) and especially in HG PMPs (fold change 0.36; $P = 0.024$).

The results of α2,3-sialylated structures were further validated by digesting the extracted acidic N-glycans with α2,3-sialidase and detecting the appearance of the digestion products in neutral N-glycan profile (Supplementary Figure 3 and Supplementary Table II). The increase in the relative abundance of multifucosylated and α2,3-sialylated glycans from normal appendices to PMPs was verified by this second method **(**Figure 5 and Supplementary Figure 4). The relative abundance of this glycan class increased from normal appendices to LAMN, to LG PMP, and to HG PMP ($P \leq 0.006$ in all comparisons) (Figure 5). Further, HG PMPs were found to show significantly higher abundance of α2,3-sialylated six N-acetylhexosamines (HexNAc) containing structures ($P = 0.020$), seven HexNAcs containing structures or larger ($P = 0.001$), large complex-type N-glycans ($P = 0.024$), fucosylated hybrid-type structures ($P = 0.001$), complex fucosylation containing hybrid-type structures ($P = 0.031$), and terminal HexNAc containing structures (bisecting-size) ($P = 0.017$) when compared to LG PMPs (Supplementary Figure 4).

Mutation profiles of the tumor specimens

To verify the mutation profiles of the LAMNs and PMP tumors, the hotspot areas of 50 cancer-related genes were analyzed with targeted next-generation sequencing (NGS). All analyzed samples were *KRAS* mutated, the most common mutation being G12D (Table I). *GNAS* mutation was detectable in 3/4 of LAMNs, in 2/4 of LG PMPs, and in 3/4 of HG PMPs, altogether present in the tumors of 6/8 (75%) of patients (Table I). All the detected *GNAS* mutations were either R201C or R201H mutation. We were not able to detect one *GNAS* mutation in a LG PMP, even if it existed in the LAMN of the same patient. A possibility exists that the LG PMP tumor represented a subclone not containing *GNAS* mutation, or that our method was not enough sensitive for the LG PMP specimen having lower tumor cell content. In addition to *KRAS* and *GNAS* mutations, three of the HG PMPs additionally contained a *TP53* mutation and one of them further contained an *ATM* mutation (Table I). For statistical analysis of the sialylation patterns in GNAS and TP53 mutated cases compared to their wild-type counterparts inside the tumor subgroups (LG or HG), our sample number was too low. When analyzed among the whole PMP sample set, no statistical differences were detected (data not shown).

Discussion

We utilized here a highly linkage-specific and repeatable protocol developed by the group of M. Wuhrer (Reiding et al. 2014) and demonstrate a significant increase in N-glycan α2,6-sialylation in PMP compared to normal appendices. Further, this increase was also significant when PMPs were compared to their appendiceal precursor lesions, i.e. LAMNs, indicating that this glycosylation alteration might be involved in the peritoneal dissemination of the tumors. Increased proportion of α2,6-sialylated glycans and, reciprocally, decreased proportion of α2,3-sialylated glycans was detected when analyzing all sialylated N-glycans, and, more specifically, in afucosylated and monofucosylated structures. This change is in line with the N-glycomic profiling study of Sethi *et al*., where paired colorectal cancers and non-neoplastic tissues were compared (Sethi et al. 2015). Indeed, increased expression of α2,6-sialylated glycans has been reported in colon cancer tissues already 30 years ago by using lectin analyses (Sata et al. 1991; Dall'Olio and Trere 1993; Yamashita et al. 1995). Further, increased levels of ST6GAL1, the predominant enzyme performing α2,6-sialylation of N-glycan's terminal galactoses, were reported in colon cancer tissues contemporarily (Dall'Olio et al. 1989; Dall'Olio et al. 2000). In addition to colorectal cancer, increased α2,6-sialylation and ST6GAL1 expression have been reported in several other cancers, and have been associated with cancer cell adhesion, migration, invasion, metastasis, therapeutic resistance, and, in fact, all the hallmarks of cancer (Lu and Gu 2015; Garnham et al. 2019). To our knowledge, this is the first report to show increased α2,6-sialylation in PMP.

Interestingly, Choi *et al*. have recently reported that increased α2,6-sialylation of endometrial cells may contribute to the spread of endometriosis into the peritoneum (Choi et al. 2018). In their study, TGF-β1-induced increase in α2,6-sialylation promoted the adhesion of endometrial cells to the mesothelial cells, and the candidate protein mediating this attachment was found to be the sialic acid-binding lectin, Siglec-9, expressed on the surface of the mesothelial cells (Choi et al. 2018). In terms of increased α2,6-sialylation in PMP, it would be exciting to study if the same phenomenon could apply to PMP, which is disseminated into the peritoneum after the initiating rupture of the appendix. In this model, TGF-β originating from the peritoneal microenvironment could up-regulate α2,6-sialylation in the tumor cells floating in the peritoneal

fluid, thereby facilitating their adhesion into the mesothelial cell layer lining the peritoneal cavity. Increased α2,6-sialylation would thus function as a driver of peritoneal dissemination. In the more studied endometriosis, an increasing number of reports demonstrate a major role for TGF-β1 in its development (Young et al. 2017). In PMP tumors, we have found highly increased expression of the TGF-β-induced protein TGFBI as compared to the control appendices (fold change 5.6) by re-analysis of the PMP microarray data published by Prof. Edward A. Levine (Levine et al. 2012; Saarinen et al. 2018). Further, highly increased plasma TGF-β has been reported in nude mice implanted with patient-derived PMP tumor fragments, as compared to the healthy ungrafted controls (Dohan et al. 2014). Both these findings thus support the involvement of TGF-β in the process of PMP outgrowth.

When sialic acid linkage types were compared according to fucosylation, increased α2,6-sialylation and decreased α2,3-sialylation were found in afucosylated and monofucosylated structures of PMPs, whereas multifucosylated structures demonstrated increased α2,3-sialylation. The reason for the opposite behavior of multifucosylated glycans originates from the acceptor substrate specificities of the glycosyltransferases involved (Figure 6). Indeed, the C6-hydroxyl group of terminal galactose, which is left free in α2,3-sialylation, is known to be essential for successful terminal fucosylation by α1,3- and α1,3/4-fucosyltransferase enzymes of both mammalian and bacterial origin (Ma et al. 2006; Shivatare et al. 2016), and α2,6-linked sialic acid can even be utilized as a protecting group to site-specifically block fucosylation in enzymatic glycan assembly (Prudden et al. 2017; Ye et al. 2019). Indeed, α2,3-sialylated structures are readily terminally fucosylated by e.g. fucosyltransferases 6 and 3 (FUT6 and FUT3) (Kannagi 2014; Kudo and Narimatsu 2014a), which are among the most frequently up-regulated FUTs in cancer (Keeley et al. 2019). Importantly, the selectin ligands sialyl-Lewis a (sLea) (also known as the tumor marker CA19-9) and sialyl-Lewis x (sLex) belong into this subclass of α2,3-sialylated and terminally fucosylated glycan structures, which is increased in PMP. In this respect, it is interesting to note that binding between sLea and E-selectin has been shown to play role in peritoneal carcinomatosis of pancreatic adenocarcinoma (Gebauer et al. 2013), and, similarly, sLex-P-selectin interaction has been shown to mediate peritoneal metastasis of ovarian cancer (Li, S. S. et al. 2019). In addition to the abundant α2,6-linked sialic acids and Siglecs, the less

abundant selectin ligands and selectins may thus additionally contribute to the peritoneal dissemination of PMP. Further, selectins are known to play role in the progression of cancer, especially in the hematogenous metastasis, where metastatic cancer cells, mimicking leukocytes, utilize selectin binding for adhesion and extravasation through endothelium (Bhide and Colley 2017). Novel anticancer therapies utilizing both siglecs and selectins are under development (Cagnoni et al. 2016).

Even if multifucosylated and α2,3-sialylated glycans increased from normal appendices to LAMNs, to LG PMP, and to HG PMP, the difference between LG and HG PMP was not statistically significant in this relatively small sample set. However, several structural subclasses of α2,3-sialylated glycans, such as large complex-type glycans and at least six HexNAcs containing glycans were significantly more abundant in the more malignant HG PMP than LG PMP. These kind of glycans could potentially serve as prognostic markers. Interestingly, FUT6, one of the enzymes central to the formation of selectin ligands, was one of the genes in the 139-gene cassette able to distinguish PMP tumors into two molecular subtypes having different prognosis, high expression of the gene cassette genes being associated with poor survival outcomes (Levine et al. 2016).

In respect to overall sialylation, the glycans of these appendiceal or appendix-originating samples mostly contained only one sialic acid, and the multisialylated structures, in turn, mostly contained only one linkage type, either α2,3- or α2,6-linkage. At single glycan level, α2,3-linkage was predominantly found in fucosylated structures, such as S1H5N4F1, and, as can be expected, in multifucosylated structures containing terminal fucose. The α2,6-linkage, in turn, was more common in afucosylated and, on the other hand, multisialylated structures (e.g. S1H5N4 and S2H5N4). This is in line with a recent report (Huang et al. 2020), demonstrating that the α2,6-sialylation performing enzyme ST6GAL1 prefers acceptor substrates without core fucosylation. The unique glycan structures presenting only one linkage type were low abundance glycans, and often they differed from the shared/unique structures of the other linkage type by just having an extra fucose, glucose, or sialic acid, and thus, the modifications were minor. The possibility, however, exists, that these low abundance molecules may still have a meaningful biological role. Especially this applies to the α2,3-sialylated and terminally fucosylated selectin ligands (Bhide and Colley 2017). One

unique α2,6-sialylated structure, S1(2.6)H3N6F2, differed from the other unique structures by being slightly more abundant and bearing multifucosylation combined with α2,6-sialylation. Based on the composition, this structure is proposed to contain two LacdiNAc (GalNAcβ1,4GlcNAc) glycan units, which are known to be frequently α2,6-sialylated in vertebrates (Stanley and Cummings 2017). The fucosyltransferase acting here could be FUT6 (Grabenhorst et al. 1998) or FUT4 (Kudo and Narimatsu 2014b), as they don't need an α2,3-sialylated acceptor glycan. In PMPs, this LacdiNAc-containing composition was significantly decreased as compared to the control appendices. Previously, the LacdiNAc glycan unit, even if being very low abundance structure in mammalian cells, has been shown to be decreased in human breast cancer, but increased in some other tumor types (e.g. prostate, ovarian, and pancreatic cancer) (Hirano et al. 2014).

In an attempt to find out if activated oncogenes could be linked to the glycosylation alterations identified, the mutation profiles of the LAMNs and the PMP tumors were analyzed by NGS. With these analyses, we found *KRAS* mutation from all the tumor specimens and *GNAS* mutation from 75.0% of the LAMN or PMP cases, which is in line with the percentages we have published earlier (Nummela et al. 2015). In addition to the common *KRAS* codon 12, 13, and 61 mutations, we further identified a rare c.34_36delinsTGG mutation, leading into G12W amino acid change. This mutation has been reported six times in the COSMIC Cataloque of Somatic Mutations in Cancer (https://cancer.sanger.ac.uk/cosmic) and all the reported cases have been colorectal adenocarcinomas or serrated adenomas. To our knowledge, this is the first time when this mutation is reported in LAMN or PMP tumor. The occurrence of all the three detected *TP53* mutations in HG tumors is in accordance with literature (Alakus et al. 2014; Nummela et al. 2015; Noguchi et al. 2015). Previously, Seales et al. have demonstrated that oncogenic ras is able to up-regulate ST6GAL1 expression in colon epithelial cells, leading to increased α2,6-sialylation of integrin β1, which, in turn, alters adhesion to collagen I (Seales et al. 2003). In our study, *KRAS* mutation was detected in both the LAMN and PMP samples, but LAMNs didn't show increase in α2,6-sialylation. KRAS mutation cannot thus solely explain the sialylation patterns observed, making the TGF-β model even more plausible.

Taken together, by sialic acid linkage analysis of PMP tissue specimens, we have identified increased

expression of α2,6-sialylated N-glycans as well as N-glycans containing multifucosylation combined with α2,3-sialylation, which both show potential to play a role in the peritoneal dissemination and progression of PMP.

Materials and methods

Tissue specimens

For N-glycan extraction, formalin-fixed, paraffin-embedded (FFPE) tissue blocks routinely prepared at the Department of Pathology, HUSLAB, Helsinki University Hospital between 2007 and 2016, were selected from four normal control appendices, four local low-grade appendiceal mucinous neoplasms (LAMN), and four low-grade (LG) and four high-grade (HG) PMP tumors. All the PMP tumors were originating from the appendix and the patients had not received preoperative oncological treatments. More detailed information of the specimens is provided in Supplementary Table III. To avoid FUT3 mutation causing discrepancies, FUT3 mutations occurring in 10% of the population (Kudo and Narimatsu 2014a), only CA19-9 immunopositive cases were included (Nummela et al. 2016).

Grading of the tumors was re-evaluated according to the WHO 2019 classification (Misdraji J, Carr NJ, Pai RK 2019) and the content of neoplastic cells was estimated by AR. According to WHO classification, LG morphology is defined by strips of cells or small islands of relatively low cellularity with typically only low-grade atypia, whereas HG morphology contains more complex structures (including invasive small cell clusters, cribriform structures and/or signet ring cell morphology), stromal reaction, and typically high-grade atypia with high cellularity (Misdraji J, Carr NJ, Pai RK 2019; Carr 2020). The proportion of HG morphology in HG specimens was ≥ 80%

To increase the epithelial cell content, macrodissection was used when cutting: areas containing the highest percentages of epithelial cells were marked on HE slides, these areas were then trimmed into the tissue block with a blade, and 10 or 30 µm thick flakes were cut from the trimmed areas. After cutting, a new HE slide was stained to confirm the representativeness of the flakes. The study was approved by the Ethics Committee

of Helsinki University Hospital.

Extraction and purification of acidic N-glycans

Before N-glycan extraction, FFPE tissue flakes were deparaffinized and disrupted in microcentrifuge tubes using a fitting plastic micro pestle. N-linked glycans were then detached by N-glycosidase F (PNGase F) digestion (Glyko; ProZyme Inc., Hayward, CA) and purified in 96-well format as previously reported (Kaprio et al. 2015; Saarinen et al. 2018). Briefly, the glycans were first passed in water through C_{18} silica and absorbed to graphitized carbon. Next, the carbon wells were washed with water and acidic glycans were eluted with 0.05% (v/v) trifluoroacetic acid in 25% (v/v) acetonitrile in water. The acidic glycans were further purified by hydrophilic interaction solid-phase extraction, after which they were finally passed in water through strong cation-exchange resin.

Ethyl esterification

To analyze the sialic acid linkage pattern, a previously developed protocol for linkage-specific sialic acid esterification was used (Reiding et al. 2014). First, acidic N-glycans were treated with 250 mM 1-ethyl-3-(3-(dimethylamino)propyl)-carbodiimide (EDAC) and 250 mM 1-hydroxybenzotriazole (HOBt) in ethanol for 1 hour at 37ºC. This resulted in ethyl esterification of α2,6-linked sialic acids, whereas α2,3-linked sialic acids instead formed a lactone with the neighboring galactose residue (Reiding et al. 2014). After the reaction, acetonitrile was added to a final concentration of 50% (v/v), and the samples were purified by hydrophilic interaction solid-phase extraction and analyzed by MALDI-TOF mass spectrometry in positive ion mode.

α2,3-sialidase digestion

To verify the α2,3-linkages of sialic acids, acidic N-glycans were separately digested with α2,3-sialidase (Glyko) overnight at 37ºC, after which they were adsorbed to porous graphitized carbon (Alltech Biotechnology, Nicholasville, KY). The miniaturized carbon columns were washed with water, and the neutral glycans were eluted with 25% acetonitrile (v/v) and the sialylated glycans with 0.05% (v/v) trifluoroacetic acid in 25% acetonitrile in water (v/v). The glycans emerging in neutral glycan profile were then analyzed with MALDI-TOF in positive ion mode.

Mass spectrometry

Matrix-assisted laser desorption-ionization time-of-flight (MALDI-TOF) mass spectrometry was performed using a Ultraflex TOF/TOF instrument (Bruker Daltonics Inc, Bremen, Germany) with acidic N-glycans detected in negative ion reflector mode as $[M-H]^-$ ions and neutral N-glycans (appearing after sialidase digestion) in positive ion reflector mode as $[M+Na]^+$ ions. The spectra were then processed into the present glycan profiles as previously (Satomaa Heiskanen Mikkola et al. 2009; Satomaa Heiskanen Leonardsson et al. 2009; Saarinen et al. 2018). The relative molar abundances of acidic and neutral glycan components were assessed based on their relative signal intensities in the spectra when analyzed separately as acidic and neutral fractions, and to allow comparison between the samples, the resulting glycan signals of the glycan profiles (acidic/neutral) were normalized to 100%. Further, the glycan components were assigned to biosynthetic groups (glycan classes) based on their proposed monosaccharide compositions (Supplementary Tables I and II) (Satomaa Heiskanen Mikkola et al. 2009; Satomaa Heiskanen Leonardsson et al. 2009; Saarinen et al. 2018).

Data analysis

As most of the detected glycan components contained only one type of sialic acid linkage, the relative abundance of glycans containing both α2,3- and α2,6-linkage being ≤ 0.8% in all the specimens, only the single linkage type glycans were used in the analyses. N-glycan data was analyzed in five different study group settings: control appendices, LAMNs, LG PMPs, and HG PMPs, as well as all PMPs (LG and HG). For statistical analyses, normal distribution of the values was first confirmed with Shapiro-Wilk test, after which two-tailed independent samples t-test or paired samples t-test (LAMN vs. LG comparisons) was used (IBM SPSS Statistics 25; IBM Corporation, Armonk, NY). $P < 0.05$ was considered as statistically significant. For correlation analysis, square of the Pearson correlation coefficient (R^2) was used.

Mutation analysis

For mutation profiling, the tumor specimens were analyzed with targeted next-generation sequencing (NGS). For that, genomic DNA was extracted from 10 µm FFPE tissue flakes after deparaffinization using a

Maxwell® 16 LEV Blood DNA Kit (Promega Corporation, Madison, WI) according to the manufacturer's instructions. Mutation hot spots areas of 50 cancer-related genes were analyzed with Ion AmpliSeq Cancer Hotspot Panel v2 (Thermo Fisher Scientific, Waltham, MA) according to the manufacturer's instructions.

Funding

This work was supported by University of Helsinki; the Sigrid Jusélius Foundation; the Finnish Cancer Foundation; Helsinki University Central Hospital Research Funds; and Finska Läkaresällskapet.

Acknowledgments

We thank Carita Liikanen and Merja Haukka for excellent technical assistance.

Conflict of interest

TS is shareholder of Glykos Finland Ltd, which performed the mass spectrometric analysis services of N-glycans. The other authors have no competing interests.

Abbreviations

FFPE, formalin-fixed, paraffin-embedded; FUT, fucosyltransferase; HexNAc, N-acetylhexosamine; HG, high-grade; LacdiNAc, N-acetyl-D-galactosamine-β1,4-N-acetyl-D-glucosamine or GalNAcβ1,4GlcNAc; LAMN, low-grade appendiceal mucinous neoplasm; LG, low-grade; MALDI-TOF, matrix-assisted laser desorption-ionization time-of-flight; NGS, next-generation sequencing; PMP, pseudomyxoma peritonei; Siglec, sialic acid-binding immunoglobulin-like lectin; sLea, sialyl-Lewis a; sLex, sialyl-Lewis x; TGF-β, transforming growth factor β

References

Alakus H, Babicky ML, Ghosh P, Yost S, Jepsen K, Dai Y, Arias A, Samuels ML, Mose ES, Schwab RB, et al. 2014. Genome-wide mutational landscape of mucinous carcinomatosis peritonei of appendiceal origin. *Genome Med*. 6:43.

Bhide GP, Colley KJ. 2017. Sialylation of N-glycans: mechanism, cellular compartmentalization and function. *Histochem Cell Biol*. 147:149-174.

Bignell M, Carr NJ, Mohamed F. 2016. Pathophysiology and classification of pseudomyxoma peritonei. *Pleura Peritoneum*. 1:3-13.

Cagnoni AJ, Perez Saez JM, Rabinovich GA, Marino KV. 2016. Turning-off signaling by Siglecs, Selectins, and Galectins: chemical inhibition of glycan-dependent interactions in cancer. *Front Oncol*. 6:109.

Carr NJ. 2020. Updates in appendix pathology: the precarious cutting edge. *Surgl Pathol Clin*. doi: 10.1016/j.path.2020.05.006.

Carr NJ, Finch J, Ilesley IC, Chandrakumaran K, Mohamed F, Mirnezami A, Cecil T, Moran B. 2012. Pathology and prognosis in pseudomyxoma peritonei: a review of 274 cases. *J Clin Pathol*. 65:919-923.

Choi HJ, Chung TW, Choi HJ, Han JH, Choi JH, Kim CH, Ha KT. 2018. Increased alpha2-6 sialylation of endometrial cells contributes to the development of endometriosis. *Exp Mol Med*. 50:1-12.

Cox EC, Thornlow DN, Jones MA, Fuller JL, Merritt JH, Paszek MJ, Alabi CA, DeLisa MP. 2019. Antibody-mediated endocytosis of polysialic acid enables intracellular delivery and cytotoxicity of a glycan-directed antibody-drug conjugate. *Cancer Res*. 79:1810-1821.

Dall'Olio F, Chiricolo M, Ceccarelli C, Minni F, Marrano D, Santini D. 2000. Beta-galactoside alpha2,6 sialyltransferase in human colon cancer: contribution of multiple transcripts to regulation of enzyme activity and reactivity with Sambucus nigra agglutinin. *Int J Cancer*. 88:58-65.

Dall'Olio F, Malagolini N, di Stefano G, Minni F, Marrano D, Serafini-Cessi F. 1989. Increased CMP-NeuAc:Gal beta 1,4GlcNAc-R alpha 2,6 sialyltransferase activity in human colorectal cancer tissues. *Int J Cancer*. 44:434-439.

Dall'Olio F, Trere D. 1993. Expression of alpha 2,6-sialylated sugar chains in normal and neoplastic colon tissues. Detection by digoxigenin-conjugated Sambucus nigra agglutinin. *Eur J Histochem*. 37:257-265.

Dohan A, Lousquy R, Eveno C, Goere D, Broqueres-You D, Kaci R, Lehmann-Che J, Launay JM, Soyer P, Bonnin P, et al. 2014. Orthotopic animal model of pseudomyxoma peritonei: an in vivo model to test anti-angiogenic drug effects. *Am J Pathol*. 184:1920-1929.

Garnham R, Scott E, Livermore KE, Munkley J. 2019. ST6GAL1: a key player in cancer. *Oncol Lett*. 18:983-989.

Gebauer F, Wicklein D, Stubke K, Nehmann N, Schmidt A, Salamon J, Peldschus K, Nentwich MF, Adam G, Tolstonog G, et al. 2013. Selectin binding is essential for peritoneal carcinomatosis in a xenograft model of human pancreatic adenocarcinoma in pfp--/rag2-- mice. *Gut*. 62:741-750.

Grabenhorst E, Nimtz M, Costa J, Conradt HS. 1998. In vivo specificity of human alpha1,3/4-fucosyltransferases III-VII in the biosynthesis of LewisX and Sialyl LewisX motifs on complex-type N-glycans. Coexpression studies from bhk-21 cells together with human beta-trace protein. *J Biol Chem*. 273:30985-30994.

Hirano K, Matsuda A, Shirai T, Furukawa K. 2014. Expression of LacdiNAc groups on N-glycans among human tumors is complex. *Biomed Res Int*. 2014:981627.

Huang G, Li Z, Li Y, Liu G, Sun S, Gu J, Kameyama A, Li W, Dong W. 2020. Loss of core fucosylation in both ST6GAL1 and its substrate enhances glycoprotein sialylation in mice. *Biochem J*. 477:1179-1201.

Järvinen P, Ristimäki A, Kantonen J, Aronen M, Huuhtanen R, Järvinen H, Lepistö A. 2014. Comparison of serial debulking and cytoreductive surgery with hyperthermic intraperitoneal chemotherapy in pseudomyxoma peritonei of appendiceal origin. *Int J Colorectal Dis*. 29:999-1007.

Kabbani W, Houlihan PS, Luthra R, Hamilton SR, Rashid A. 2002. Mucinous and nonmucinous appendiceal adenocarcinomas: different clinicopathological features but similar genetic alterations. *Mod Pathol*. 15:599-605.

Kannagi R. 2014. Fucosyltransferase 6. GDP-fucose lactosamine α3-fucosyltransferase (FUT6). In: Taniguchi N, Honke K, Fukuda M, Narimatsu H, Yamaguchi Y, Angata T, editors. *Handbook of Glycosyltransferases and Related Genes*. Tokyo, Japan: Springer. p. 559-571.

Kaprio T, Satomaa T, Heiskanen A, Hokke CH, Deelder AM, Mustonen H, Hagström J, Carpen O, Saarinen J, Haglund C. 2015. N-glycomic profiling as a tool to separate rectal adenomas from carcinomas. *Mol Cell Proteomics*. 14:277-288.

Keeley TS, Yang S, Lau E. 2019. The diverse contributions of fucose linkages in cancer. *Cancers (Basel)*. 11:1241.

Kudo T, Narimatsu H. 2014a. Fucosyltransferase 3. GDP-fucose lactosamine α1,3/4-fucosyltransferase. Lea and Leb histo-blood groups (FUT3, Lewis enzyme). In: Taniguchi N, Honke K, Fukuda M, Narimatsu H, Yamaguchi Y, Angata T, editors. *Handbook of Glycosyltransferases and Related Genes*. Tokyo, Japan: Springer. p. 531-539.

Kudo T, Narimatsu H. 2014b. Fucosyltransferase 4. GDP-fucose lactosamine α1,3-fucosyltransferase. myeloid specific (FUT4). In: Taniguchi N, Honke K, Fukuda M, Narimatsu H, Yamaguchi Y, Angata T, editors. *Handbook of Glycosyltransferases and Related Genes*. Tokyo, Japan: Springer. p. 541-547.

Levine EA, Blazer DG, Kim MK, Shen P, Stewart JH, Guy C, Hsu DS. 2012. Gene expression profiling of peritoneal metastases from appendiceal and colon cancer demonstrates unique biologic signatures and predicts patient outcomes. *J Am Coll Surg*. 214:599-7.

Levine EA, Votanopoulos KI, Qasem SA, Philip J, Cummins KA, Chou JW, Ruiz J, D'Agostino R, Shen P, Miller LD. 2016. Prognostic molecular subtypes of low-grade cancer of the appendix. *J Am Coll Surg*. 222:493-503.

Li F, Ding J. 2019. Sialylation is involved in cell fate decision during development, reprogramming and cancer progression. *Protein Cell*. 10:550-565.

Li SS, Ip CKM, Tang MYH, Tang MKS, Tong Y, Zhang J, Hassan AA, Mak ASC, Yung S, Chan TM, et al. 2019. Sialyl Lewis(x)-P-selectin cascade mediates tumor-mesothelial adhesion in ascitic fluid shear flow. *Nat Commun*. 10:2406-6.

Lu J, Gu J. 2015. Significance of beta-galactoside alpha2,6 sialyltranferase 1 in cancers. *Molecules*. 20:7509-7527.

Ma B, Simala-Grant JL, Taylor DE. 2006. Fucosylation in prokaryotes and eukaryotes. *Glycobiology*. 16:158R-184R.

Mereiter S, Balmana M, Campos D, Gomes J, Reis CA. 2019. Glycosylation in the era of cancer-targeted therapy: where are we heading? *Cancer Cell*. 36:6-16.

Mereiter S, Balmana M, Gomes J, Magalhaes A, Reis CA. 2016. Glycomic approaches for the discovery of targets in gastrointestinal cancer. *Front Oncol*. 6:55.

Misdraji J, Carr NJ, Pai RK. 2019. Appendiceal mucinous neoplasm. In: WHO classification of tumours editorial board. *Digestive system tumours, WHO classification of tumours,* 5th edition. Lyon, France: IACR. p. 144-146.

Mittal R, Chandramohan A, Moran B. 2017. Pseudomyxoma peritonei: natural history and treatment. *Int J Hyperthermia*. 33:511-519.

Noguchi R, Yano H, Gohda Y, Suda R, Igari T, Ohta Y, Yamashita N, Yamaguchi K, Terakado Y, Ikenoue T, et al. 2015. Molecular profiles of high-grade and low-grade pseudomyxoma peritonei. *Cancer Med*. 4:1809-1816.

Nummela P, Leinonen H, Järvinen P, Thiel A, Järvinen H, Lepistö A, Ristimäki A. 2016. Expression of CEA, CA19-9, CA125, and EpCAM in pseudomyxoma peritonei. *Hum Pathol*. 54:47-54.

Nummela P, Saarinen L, Thiel A, Järvinen P, Lehtonen R, Lepistö A, Järvinen H, Aaltonen LA, Hautaniemi S, Ristimäki A. 2015. Genomic profile of pseudomyxoma peritonei analyzed using next-generation sequencing and immunohistochemistry. *Int J Cancer*. 136:282.

Patrick-Brown, T D J H, Carr NJ, Swanson DM, Larsen S, Mohamed F, Flatmark K. 2020. Estimating the prevalence of pseudomyxoma peritonei in Europe using a novel statistical method. *Ann Surg Oncol*. doi: 10.1245/s10434-020-08655-8.

Pinho SS, Reis CA. 2015. Glycosylation in cancer: mechanisms and clinical implications. *Nat Rev Cancer*. 15:540-555.

Prudden AR, Liu L, Capicciotti CJ, Wolfert MA, Wang S, Gao Z, Meng L, Moremen KW, Boons GJ. 2017. Synthesis of asymmetrical multiantennary human milk oligosaccharides. *PNAS*. 114:6954-6959.

Reiding KR, Blank D, Kuijper DM, Deelder AM, Wuhrer M. 2014. High-throughput profiling of protein N-glycosylation by MALDI-TOF-MS employing linkage-specific sialic acid esterification. *Anal Chem*. 86:5784-5793.

Saarinen L, Nummela P, Leinonen H, Heiskanen A, Thiel A, Haglund C, Lepistö A, Satomaa T, Hautaniemi S, Ristimäki A. 2018. Glycomic profiling highlights increased fucosylation in pseudomyxoma peritonei. *Mol Cell Proteomics*. 17:2107-2118.

Saarinen L, Nummela P, Thiel A, Lehtonen R, Järvinen P, Järvinen H, Aaltonen LA, Lepistö A, Hautaniemi S, Ristimäki A. 2017. Multiple components of PKA and TGF-beta pathways are mutated in pseudomyxoma peritonei. *PLoS One*. 12:e0174898.

Sata T, Roth J, Zuber C, Stamm B, Heitz PU. 1991. Expression of alpha 2,6-linked sialic acid residues in neoplastic but not in normal human colonic mucosa. A lectin-gold cytochemical study with Sambucus nigra and Maackia amurensis lectins. *Am J Pathol*. 139:1435-1448.

Satomaa T, Heiskanen A, Leonardsson I, Ångström J, Olonen A, Blomqvist M, Salovuori N, Haglund C, Teneberg S, Natunen J, et al. 2009. Analysis of the human cancer glycome identifies a novel group of tumor-associated N-acetylglucosamine glycan antigens. *Cancer Res*. 69:5811-5819.

Satomaa T, Heiskanen A, Mikkola M, Olsson C, Blomqvist M, Tiittanen M, Jaatinen T, Aitio O, Olonen A, Helin J, et al. 2009. The N-glycome of human embryonic stem cells. *BMC Cell Biol*. 10:42.

Schneider M, Al-Shareffi E, Haltiwanger RS. 2017. Biological functions of fucose in mammals. *Glycobiology*. 27:601-618.

Seales EC, Jurado GA, Singhal A, Bellis SL. 2003. Ras oncogene directs expression of a differentially sialylated, functionally altered beta1 integrin. *Oncogene*. 22:7137-7145.

Sethi MK, Kim H, Park CK, Baker MS, Paik YK, Packer NH, Hancock WS, Fanayan S, Thaysen-Andersen M. 2015. In-depth N-glycome profiling of paired colorectal cancer and non-tumorigenic tissues reveals cancer-, stage- and EGFR-specific protein N-glycosylation. *Glycobiology*. 25:1064-1078.

Shetty S, Thomas P, Ramanan B, Sharma P, Govindarajan V, Loggie B. 2013. Kras mutations and p53 overexpression in pseudomyxoma peritonei: association with phenotype and prognosis. *J Surg Res*. 180:97-103.

Shivatare SS, Chang SH, Tsai TI, Tseng SY, Shivatare VS, Lin YS, Cheng YY, Ren CT, Lee CCD, Pawar S,et al. 2016. Modular synthesis of N-glycans and arrays for the hetero-ligand binding analysis of HIV antibodies. *Nat Chem*. 8:338-346.

Stanley P, Cummings RD. 2017. Structures common to different glycans. In: Varki A, Cummings RD, Esko JD, Stanley P, Hart GW, Aebi M, Darvill AG, Kinoshita T, Packer NH, Prestegard JH, Schnaar RL, Seeberger PH, editors. *Essentials of glycobiology*, 3rd edition. Cold Spring Harbor (NY): Cold Spring Harbor Laboratory Press. p.161-178.

Sugarbaker PH, Kern K, Lack E. 1987. Malignant pseudomyxoma peritonei of colonic origin. Natural history and presentation of a curative approach to treatment. *Dis Colon Rectum*. 30:772-779.

Yamashita K, Fukushima K, Sakiyama T, Murata F, Kuroki M, Matsuoka Y. 1995. Expression of Sia alpha 2-->6Gal beta 1-->4GlcNAc residues on sugar chains of glycoproteins including carcinoembryonic antigens in human colon adenocarcinoma: applications of Trichosanthes japonica agglutinin I for early diagnosis. *Cancer Res*. 55:1675-1679.

Ye J, Xia H, Sun N, Liu CC, Sheng A, Chi L, Liu XW, Gu G, Wang SQ, Zhao J, et al. 2019. Reprogramming the enzymatic assembly line for site-specific fucosylation. *Nat Catal*. 2:514-522.

Young VJ, Ahmad SF, Duncan WC, Horne AW. 2017. The role of TGF-beta in the pathophysiology of peritoneal endometriosis. *Hum Reprod Update*. 23:548-559.

Legends to figures

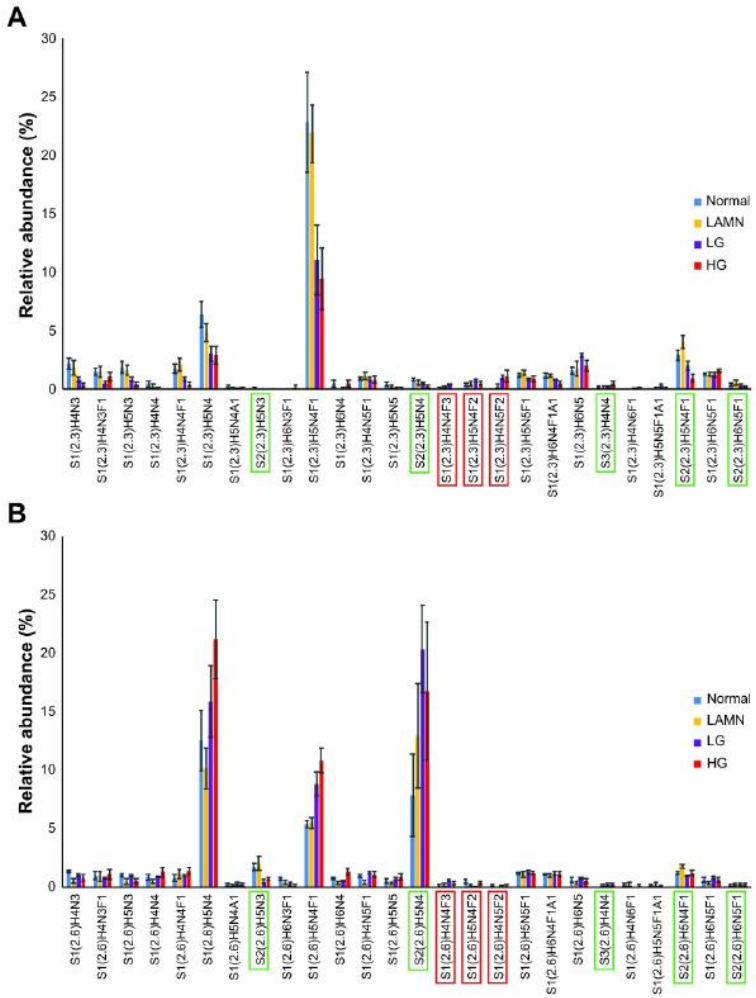

Figure 1. Shared α2,3- and α2,6-sialylated structures. Relative abundance of acidic monosaccharide compositions in normal appendix controls (blue bars), in low-grade appendiceal mucinous neoplasms (LAMNs, yellow bars), and in pseudomyxoma peritonei (PMP) samples of low-grade (LG, purple bars) and of high-grade (HG, red bars) as analyzed by ethyl esterification combined with MALDI-TOF mass spectrometry (n = 4 in each sample group). On x-axis are shown the proposed acidic N-glycan compositions subdivided into α2,3-sialylated (**A**) and α2,6-sialylated (**B**) forms. The results are shown as means ±SEM. H = Hexose; N = N-Acetylhexosamine; F = Deoxyhexose; S = Sialic acid; A = Acetylated. Red rectangles represent multifucosylated structures (F > 1), and green rectangles represent multisialylated structures (S > 1).

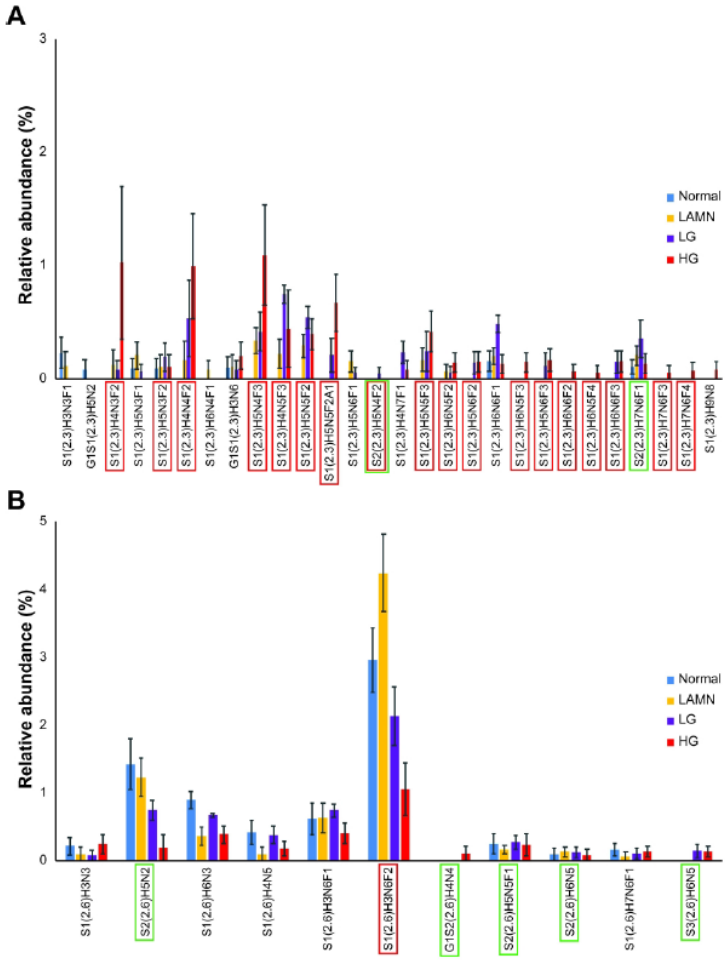

Figure 2. Unique α2,3- or α2,6-sialylated structures. Relative abundance of acidic monosaccharide compositions in normal appendix controls (blue bars), in low-grade appendiceal mucinous neoplasms (LAMNs, yellow bars), and in pseudomyxoma peritonei (PMP) samples of low-grade (LG, purple bars) and of high-grade (HG, red bars) as analyzed by ethyl esterification combined with MALDI-TOF mass spectrometry (n = 4 in each sample group). On x-axis are shown the proposed acidic N-glycan compositions subdivided into unique α2,3-sialylated structures (**A**) and unique α2,6-sialylated structures (**B**). The results are shown as means ±SEM. H = Hexose; N = N-Acetylhexosamine; F = Deoxyhexose; S = Sialic acid; G = Glucose; A = Acetylated. Red rectangles represent multifucosylated structures (F > 1), and green rectangles represent multisialylated structures (S > 1).

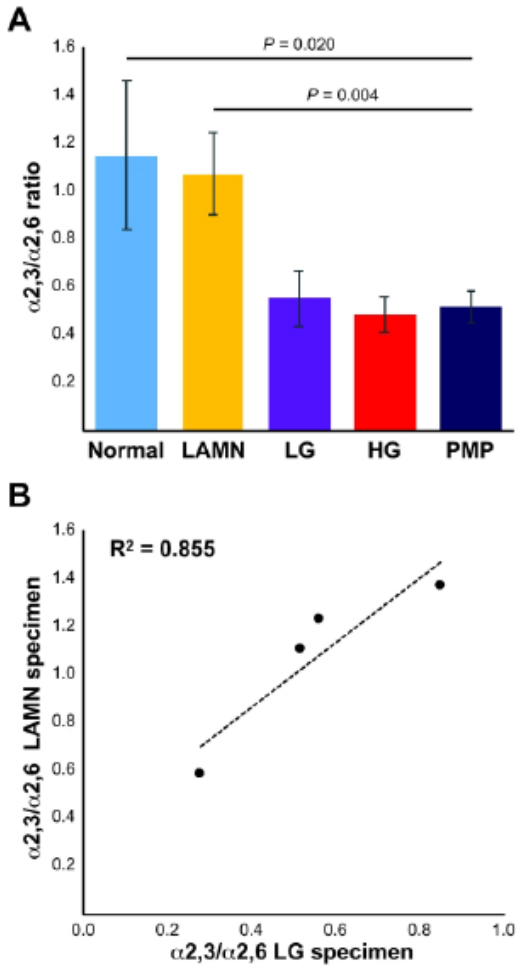

Figure 3. Ratio of α2,3- and α2,6-sialylation. **A)** Ratio of α2,3/α2,6-sialylation in normal appendix controls (middle blue bar), in low-grade appendiceal mucinous neoplasms (LAMNs, yellow bar), in pseudomyxoma peritonei (PMP) samples of low-grade (LG, purple bar) and of high-grade (HG, red bar), and in all PMP samples (LG + HG, dark blue bar). The values are means ±SEM. **B)** The α2,3/α2,6-ratios of the paired LAMN and LG PMP specimens show strong correlation (R^2 = 0.855).

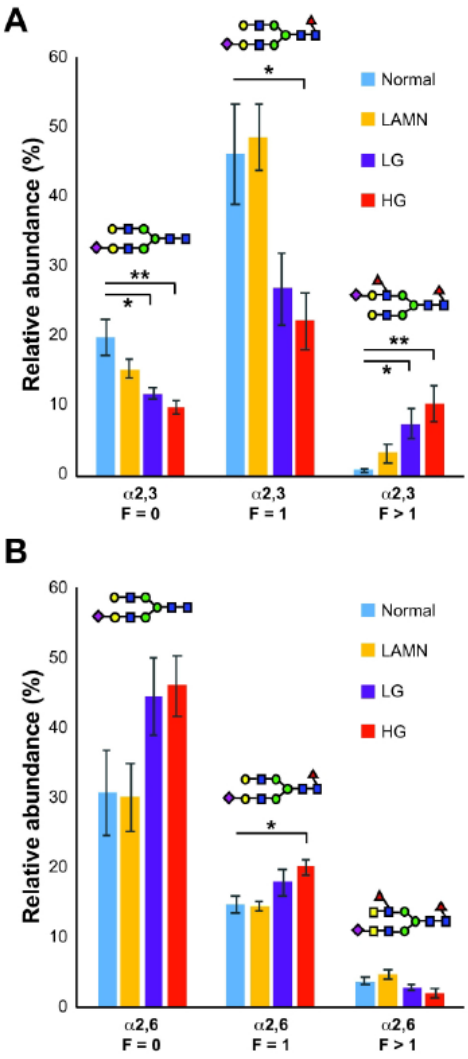

Figure 4. Sialylation in respect to fucosylation. Relative abundance of α2,3- (**A**) and α2,6-sialylated (**B**) glycan structures is subgrouped into afucosylated (F = 0), monofycosylated (F = 1), and multifucosylated (F > 1) ones. A representative structure is shown on top of each subgroup depicted by blue square (N-acetyl-D-glucosamine), green circle (D-mannose), yellow circle (D-galactose), yellow square (N-acetyl-D-galactosamine), red triangle (L-fucose), and purple diamond (sialic acid, more specifically N-acetylneuraminic acid). Blue bars represent normal appendices, yellow bars low-grade appendiceal mucinous neoplasms (LAMN), purple bars low-grade (LG) pseudomyxoma peritonei (PMP) tumors, and red bars high-grade (HG) PMP tumors (n = 4 in each group). The values are means ±SEM. *$P < 0.03$, **$P \leq 0.01$.

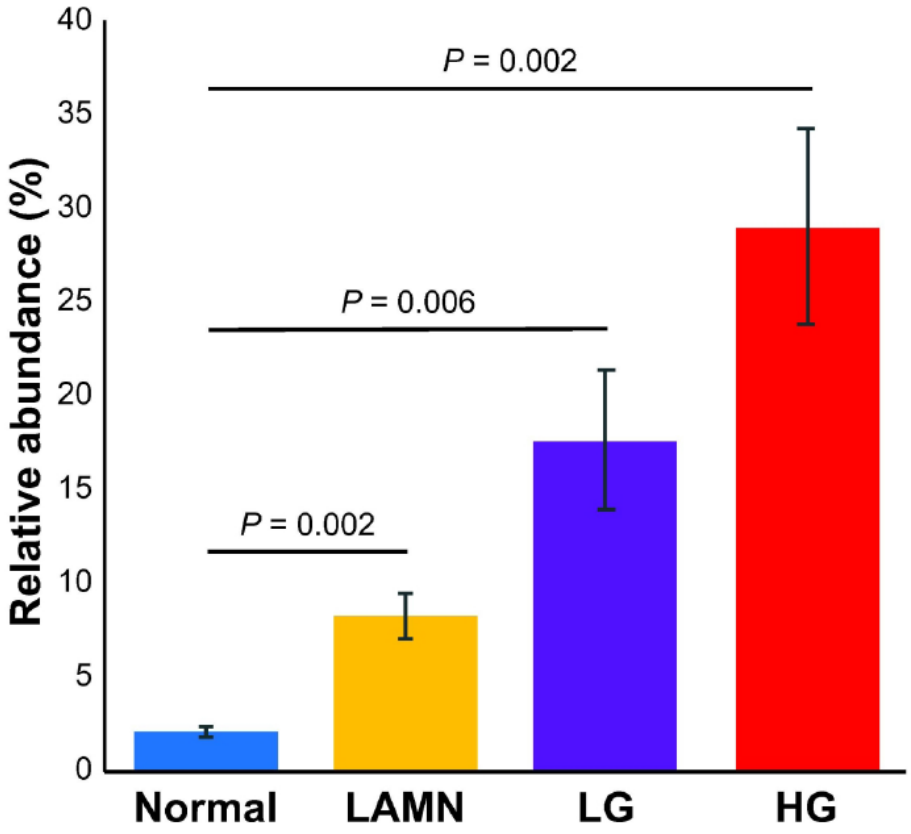

Figure 5. α2,3-sialylation combined with multifucosylation. Relative abundance of α2,3-sialylated and multifucosylated glycan structures additionally analyzed as structures appearing in neutral N-glycan profile after α2,3-sialidase digestion of acidic N-glycans. Blue bar represent normal appendices, yellow bar low-grade appendiceal mucinous neoplasms (LAMN), purple bar low-grade (LG) pseudomyxoma peritonei (PMP) tumors, and red bar high-grade (HG) PMP tumors (n = 4 in each group). The values are means ±SEM.

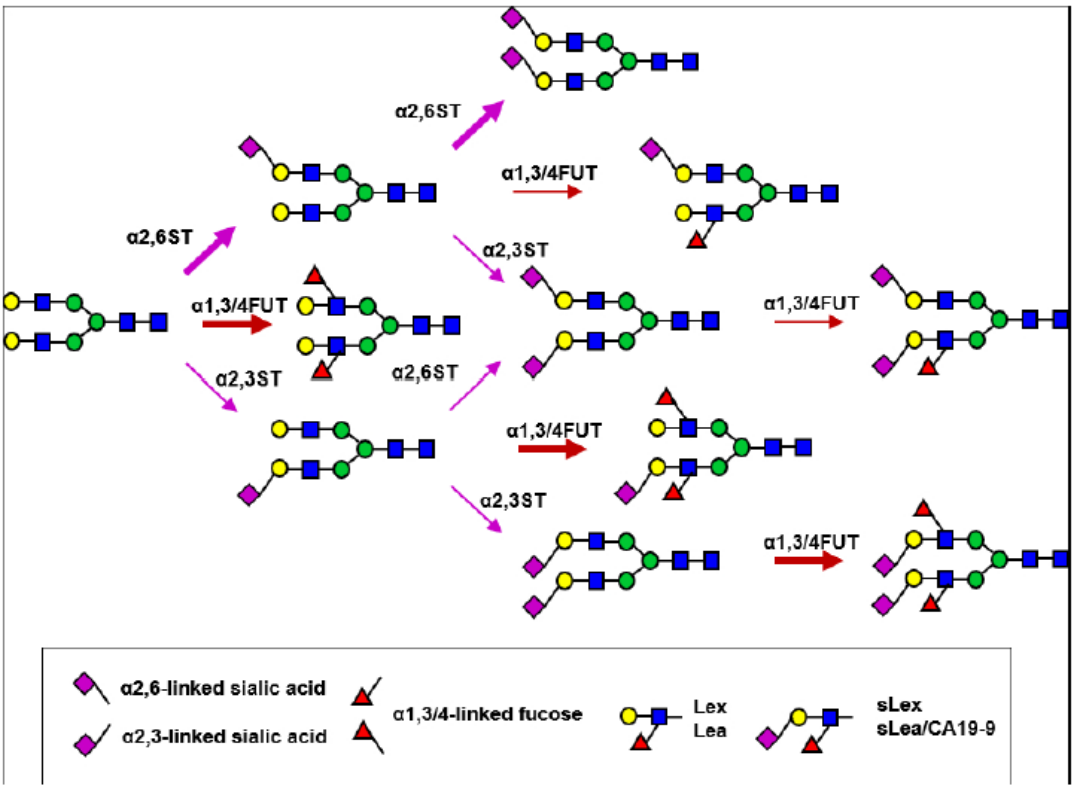

Figure 6. Schematic representation of plausible sialylated and fucosylated N-glycan structures and their synthesis in PMP. Two main biosynthetic rules apply: 1) fucosylated N-glycan antennae are not further sialylated and 2) α2,6-sialylated antennae are not further fucosylated, leading to the biosynthetic pathways as outlined here. Bolded arrows show observed main routes to sialylated and fucosylated glycans in PMP. Only biantennary complex-type N-glycans are shown and core-fucosylated as well as α1,2-fucosylated structures have been omitted for clarity. Monosaccharide symbols: blue square (N-acetyl-D-glucosamine), green circle (D-mannose), yellow circle (D-galactose), red triangle (L-fucose), and purple diamond (sialic acid, more specifically N-acetylneuraminic acid).

Table I. Mutation profiles of the analyzed tumor specimens

Specimen		KRAS		GNAS		TP53		ATM	
Code	Type	Mutation	Frequency (%)	Mutation	Frequency (%)	Mutation	Frequency (%)	Mutation	Frequency (%)
L2	LAMN	G12D	30	R201C	18				
L6	LAMN	Q61H	4	R201H	7				
L213	LAMN	G12C	9	R201H	11				
L287	LAMN	G12W[b]	10						
mL2A	LG	G12D	17						
mL6	LG	Q61H	4	R201H	7				
mL213	LG	G12C	14	R201H	4				
mL287	LG	G12W[b]	3						
Hb[a]	HG	G13D	25	R201C	8				
H30	HG	G12D	24	R201H	20	C135Y	10		
H303	HG	G12V	18			Y163Hfs*4[c]	37		
H305	HG	G12D	30	R201C	25	P151R	38	G2695A	17

[a]Mutations of the specimen Hb were from our previous study (Nummela et al. 2015).

[b]*KRAS* G12W mutation was more specifically c.34_36delinsTGG.

[c]*TP53* Y163Hfs*4 mutation was more specifically c.486_495del.

LAMN, low-grade appendiceal mucinous neoplasm; LG, low-grade pseudomyxoma peritonei; HG, high-grade pseudomyxoma peritonei.